MiR-106b-5p represses neuropathic pain by regulating P2X4 receptor in the spinal cord in mice

Huiying Du

  Second Affiliated Hospital of Guangzhou Medical College

Xinran Tan

  The Second Affiliated Hospital of Guangzhou Medical University

Xuhong Wei

  The Second Affiliated Hospital of Guangzhou Medical University

Zhongmin Yuan

  The Second Affiliated University of Guangzhou Medical University

Qingjuan Gong (✉ gqj01@sohu.com)

Abstract

Background: P2X$_4$ receptor (P2X$_4$R)-mediated spinal microglial activation makes a critical contribution to pathologically enhanced pain processing in the dorsal horn. It can be upregulated under conditions of neuropathic pain. However, the specific mechanism of pathogenesis and potential molecular targets has not yet been made explicit. MicroRNAs (miRNAs) are commonly recognized as indicators in neuropathic pain pathophysiology.

Methods: We established the pain model of spared nerve injury (SNI), and the 50% paw withdrawal thresholds (PWMTs) were used to assess behavior of mouse. MiRNA expression profiling was performed to detect differential expressed miRNA. The western-bolt and quantitative real time PCR to examine P2X4R and miRNA expression in the mouse. Dual-luciferase reporter assays confirmed the correlation between P2X4R and miRNA. Fluorescence in situ hybridization was used to show location between P2X4R and miRNA.

Results: In the present study, we found that P2X$_4$R was up-regulated in the spinal dorsal horn of mice following spared nerve injury (SNI), and we identified 69 miRNAs (46 up-regulated and 23 down-regulated miRNAs) were differently expressed (fold change > 2, P < 0.05). P2X$_4$R was a major target of miR-106b-5p (one of down-regulated miRNAs in SNI) with bioinformatics technology and quantitative real time PCR analysis validated the expressed change of miR-106b-5p, and dual-luciferase reporter assays confirmed the correlation between them. Fluorescence in situ hybridization showed that miR-106b-5p was co-localized with P2X$_4$R in the spinal cord. Transfection with miR-106b-5p mimic on BV2 cells reversed the up-regulation of P2X$_4$R induced by LPS. Moreover, miR-106b-5p overexpression significantly attenuated neuropathic pain induced by SNI, with decreased expression of P2X$_4$R mRNA and protein in the spinal cord.

Conclusion: Taken together, our results suggest that miR-106b-5p can serve as an important regulator of neuropathic pain development by targeting P2X$_4$R.

Introduction

Pain is defined as an unpleasant sensory and emotional experience associated with actual or potential tissue damage by the International Association for the Study of pain [1], and neuropathic pain is defined as "pain caused by a lesion or disease of the somatosensory nervous system" [2]. Neuropathic pain treatment is a great challenge and the outcomes remain unsatisfactory, mainly due to barely understood pathogenesis and a lack of well-defined molecular targets [3, 4].

P2X receptors are non-selective cation channels that open in response to adenosine triphosphate (ATP) binding, allowing the rapid flow of ions (K$^+$, Na$^+$, Ca^{2+}) across the membrane [5]. Among the seven P2X receptors, P2X$_4$ receptor (P2X$_4$R) display the most widespread tissue distribution and expression in neurons and the immune system [6]. Studies have found that P2X$_4$R is closely related to the immune system and plays vital functions through monocytes, macrophages, dendritic cells, neutrophils, and T lymphocytes [7]. Purinergic receptor-mediated spinal microglial functions make a critical role in pain processing [8, 9]. A great deal of evidence has shown that P2X$_4$R plays a vital role in the process of neuropathic pain [10, 11]. Our previous study has found that ATP activates p38 mitogen-activated protein kinase (p38 MAPK) by binding to endogenous P2X$_4$R in

microglia and subsequently increases the expression of P2X$_4$R, thus promoting long-term potentiation [12], which is the basis of the hypersensitization of nociceptive neurons in the spinal cord. A previous study demonstrated that the blockade of P2X$_4$R inhibits neuropathic pain-related behavior by preventing MMP-9 activation, then pronociceptive interleukins (IL- 1β, IL-18, IL-6) release in CCI-induced rat model, suggesting that P2X$_4$R may indeed play a significant role in neuropathic pain development by modulating neuroimmune interactions in the spinal cord and DRG [11]. Although these studies have partly elucidated the mechanism of altered P2X$_4$R expression, the specific mechanism are not complete clear.

MiRNAs are highly deregulated in neuropathic pain, and might be a critical molecule for treatment [13, 14]. MiRNAs can negatively regulate gene expression by translationally targeting the targeted mRNAs [15–17], and can serve as indicators in neuropathic pain pathophysiology [18–20]. It has been found that miR-98 might depress neuropathic pain development through modulating high mobility group AT-hook 2 (HMGA2) [21] and that miR-30b is involved in the development of neuropathic pain, probably by regulating the expression of Nav1.3 [3]. However, whether miRNA is involved in the pathogenesis of neuropathic pain by regulating the P2X$_4$R has not been discovered. In the present study, P2X$_4$R was up-regulated and a microarray analysis was constructed to identify differential expressed (DE) miRNAs in the spinal dorsal horn following spared nerve injury (SNI). Moreover, the interaction of potential miRNA and P2X$_4$R was evaluated to clarify the underlying mechanisms involved in the development of neuropathic pain.

Materials And Methods
Animals

Male Balb/c mice aged 8 weeks were purchased from Animal Experimental Center, Sun Yat-sen University, China (Guangzhou, China). Mice were housed in separated cages and the rooms were kept at 24 ± 1°C (297 ± 1 K) temperature and 50–60% humidity, under a 12/12 light-dark cycle and with free access to food and water ad libitum. All experimental procedures were approved by the Institutional Animal Care and Use Committee of Guangzhou Medical University and were carried out in accordance with the guidelines of the National Institutes of Health on animal care and the ethical guidelines for investigation of experimental pain in conscious animal.

Cell Culture And Transfection

Culture and transfection of BV2 cells were carried out as described elsewhere [22]. All cells were collected in high glucose Medium (Gibco) with 10% FBS (JRScientific, Woodland, CA, USA), 100 mg/mL streptomycin, and 100 units/mL penicillin (Quality Biological, Gaithersburg, MD, USA). The cells were incubated at 37 C, 95% O2, and 5% CO2 with a seeding density of 1*10^5 BV2 cells/mL. One day later, miRNAs mimic or inhibitor (RiboBio, Guangzhou, China) were transfected in the cells. 120 ul Opti-Mem was used to dilute miR-106b-5p mimic (50 nM)/inhibitor (100 nM) or negative control. The sequences for miR-106b-5p mimic are as follow, forward: 5-UAAAGUGCUGACAGUGCAGAU-3, Reverse: 5-AUUUCACGACUGUCACGUCUA-3; the sequences for miR-106b-5p inhibitor is 5-AUUUCACGACUGUCACGUCUA-3. The final concentrations of mimic and inhibitor were 50 nM and 100 nM, respectively. 120 ul Opti-Mem was simultaneously used to dilute 7.5 uL RNAiMAX (Invitrogen, Carlsbad, CA), then the two solutions were mixed. After 5 min, the mixture was placed into each 2 mL well and

high glucose medium was added. 2 ml LPS (100 ng/mL, Sigma) was added to each 2 mL well 6 h before the the cells were collected 48 h later for qPCR and western-blot examinations.

Cell Proliferation Assay

Cell proliferation was evaluated using a cell counting kit-8 (CCK-8) assay (Beyotime, China). BV2 cells (5×10^3) were plated onto 96-well plates, then the LPS or miRNA mimic or miRNA inhibitor were added in the BV2 cells. Each well contained 100 μL of medium supplemented with 10 μL of CCK8 solution. The absorbance at 450 nm was measured to assess the degree of cell proliferation after incubating the cells at 37 °C for 1 hr.

Luciferase Assay

A dual luciferase reporter assay was performed as outlined for a previous procedure [23]. The pmirGLO dual-luciferase vector (pmirGLO vector), which contained both the firefly luciferase gene and the renilla luciferase gene, was purchased from Promega (Madison, WI, USA). $P2X_4R$ 3'UTR, including the predicted binding sites of miR-106b-5p, was inserted into the 3'UTR region downstream of the firefly luciferase gene of the pmirGLO vector (pmir-GLO-UTR). HEK293 cells were cultivated in high glucose medium (Gibco) with 10% FBS (JRScientific, Woodland, CA, USA), 100 mg/mL streptomycin, and 100 units/mL penicillin (Quality Biological, Gaithersburg, MD, USA). The cells were incubated in a humidified incubator with 5% CO2 at 37°C. When the HEK293T cells had a confluency of 70–80%, A $P2X_4R$-luciferase-reporter construct (pmiRGLO-$P2X_4R$ 3'-UTR vector), containing the miR-106b-5p binding motif, was co-transfected with miR-106b-5p mimic at different doses of 10, 20, and 50 nM (20 umol/L) or NC mimic into HEK293 cells by using RNAiMAX (Invitrogen). After another 48 h of culture, we used 1 * passive lysis buffer to lyse the transfected cells, and 20 ul supernatant was achieved for luciferase activity using the Dual-Luciferase Reporter Assay System (Promega). The ratio of firefly activity to renilla activity was recognized as relative reporter activity. Experiments were performed in triplicate and repeated three times.

Surgical Procedures And Drug Infusion

SNI surgeries were performed to mice according to our previous work [24]. In brief, mice were deeply anesthetized after the behavioral tests. The skin of the lateral thigh was incised and the biceps femoris muscle was dissected bluntly to expose the left sciatic nerve and its three terminal branches (the sural, common peroneal and tibial nerves). The common peroneal and the tibial nerves were tightly ligated with 5 – 0 silk. Then, the nerve was transected distal to the ligation, and 2–4 mm length of nerve fiber was removed. Great care was taken to avoid any contact with or stretching of the intact sural nerve. The wound was closed in two layers. The sham group was given all procedures except ligation and transection.

The method of intrathecal injections was described previously [25]. In brief, mice were restrained with the left hand and the injection was performed with the right hand. The vertebral landmarks for L5 and L6 vertebrate were identified by palpation. An injection into the subarachnoid space between the L5 and the L6 vertebrae was done via a 27-gage needle. Entry of the needle was confirmed with the presence of a tail flick. The injection

volume of all other compounds was 5 μl. In on part, the mice were divided into three groups: sham + scramble (saline), SNI + scramble (saline) and SNI + miR-106b-5p agomir (a selective mimic of miR-106b-5p). In another part, the mice were divided into two groups, naïve + scramble and naïve + miR-106b-5p antagomir. Beginning 1 day after naïve or 7 days after SNI surgery, continuous intrathecal infusion was delivered once a day for 3 days, from day 1 to 3 for naïve mice and from day 7 to 9 for SNI mice. Mice with neurological deficits were excluded from the experiment.

Behavior Tests

The 50% paw withdrawal thresholds (PWMTs) were measured on days 0, 3, 5, and 7 for the evaluation of SNI model or on days 0, 5, 7, 8, 9, 10, and 14 during continuous miR-106b-5p agomir injection following SNI surgery. They were measured on days 0, 1, 2, and 3 during continuous miR-106b-5p antagomir injection in naïve mice, always between 8 and 10 AM in the morning. PWMT was assessed with method described previously [26]. The filament force evoking paw withdrawals for more than 3 times in a round of testing was defined as the mechanical threshold. The cutoff force was 4 g. The observation of a positive response (paw lifting, shaking, or licking) within 5 s.

Mirna Microarray Analysis

The method was described as our previous study [13]. MiRNA expression profiling was performed using the RiboArray platform (RiboBio, Guangzhou, China). In brief, 1 lg of total RNA was labeled with a Cy3 using a ULS™ microRNA Labeling Kit (Kreatech, Amsterdam, Netherlands) and hybridized on the microarray. Based on Sanger miRBase version 19.0 database, RiboBio designed 1263 specific oligos for 1281 mouse miRNA, where 1263 are non-redundant sequence. In addition, 54 RiboArray™ internal controls were used. We also put some probes for location identify function. T-test P-value of < 0.05 and fold-change (> 2) were applied to determine two differentially expressed (DE) sets of genes of six experimental samples.

Rna Extraction And Quantitative Real Time Pcr (qpcr)

Total RNA was extracted using the Trizol method [24, 27]. The quality and quantity of RNA were measured using a Nanodrop Spectrophotometer (Thermo Scientific) and samples with an absorbance ratio at 260/280 between 1.8–2.2 were considered acceptable. RNA degradation was not assessed. RNA dilutions were made up in nuclease-free water. For analysis of mRNA, the method was described previously [24, 27]. Reverse transcription was generated using the SuperScriptTM III Reverse Transcriptase (Invitrogen) with a Gene Amp PCR System 9700 (Applied Biosystems). For miRNA analysis, 1 ug RNA was used for reverse transcription by miRNA 1st Strand cDNA Synthesis Kit (by stem-loop) (Vazyme, #MR101) according to the instructions. Quantitative Real-time PCR (qPCR) was carried out on a real-time detection instrument ViiA 7 Real-time PCR System (Applied Biosystems) using 2X PCR master mix (Arraystar). All experiments were replicated three times. The relative expression of genes was calculated based on the $2^{-\triangle\triangle Ct}$ method using the mouse housekeeping GAPDH/U6 gene as an endogenous control. Expression ratios were subjected to a log2 transform to produce fold change data.

Western Blot

To ensure a sufficient amount of protein, BV2 cells and a section of ipsilateral Lumbar enlargement was prepared. Based on established protocol [28], tissues were homogenized in a RIPA buffer (Sangon, Shanghai, China). After centrifugation at 12 000 × g for 15 min at 4 °C, the supernatant was collected to analyze cytosolic proteins, and protein concentrations were determined with a BCA Kit (Thermo Fisher Scientific, Rockford, IL, USA). The contents of the proteins in the samples were measured using the Bio-Rad protein assay (Bio-Rad) and were then heated at 99 °C for 5 min. Samples of 20 mg total protein were separated by 10% SDS-polyacrylamide gel electrophoresis and electrophoretically transferred onto a polyvinylidene difluoride membrane. After the membranes were blocked with 5% Milk in Tris-buffered PBS containing 0.1% Tween-20 for 1 h, then rabbit anti-P2X$_4$R (1:1000, Alomone Labs), rabbit anti-tubulin (1:10000, Sigma), and rabbit anti-GAPDH (1:5000, Cell Signaling Technology) primary antibodies would be used. The proteins were detected using horseradish peroxidase-conjugated anti-rabbit secondary antibody (1:1000, Jackson) and visualized using Western peroxide reagent and luminol/enhancer reagent (Clarity Western ECL Substrate, Bio-Rad). The intensity of the blots was quantified via densitometry using Image J software. All cytosol protein bands were normalized to tubulin or GAPDH.

Fluorescence In Situ Hybridization

The fluorescence in situ hybridization technology was performed by Servicebio (wuhan, China). The spinal cord of animals was sectioned at 3 mm, and sections were dehydrated in series of ethanol washes (70%, 85%, and 100%) and air-dried. After incubated in hybridization solution at 37 °C for 1 h, the sections were incubated overnight in hybridization solution with 6 ng/µL of DIG (488) labeled probes for miR-106b-5p (5'-DIG-ATCTGCACTGTCAGCACTTTA-DIG-3') at 37 °C. Following hybridization, the sections were washed twice at 37 °C with 2 × SSC for 10 min, then twice at 37 °C with 1 × SSC for 5 min and in 0.5 × SSC at room temperature for 10 min. After they were blocked for 30 min at room temperature, we incubated them with anti-DIG-HRP at 37 °C for 50 min. Finally, FITC-TSA was added at dark for 5 min. To identify the cell types expressing miR-106b-5p, the above sections were incubated overnight at 4 °C with primary antibodies against ATP-gated cation channel protein (P2X$_4$R, rabbit, 1:100,), the ionized calcium-binding adapter molecule (IBA-1, rabbit, 1:300;), glial fibrillary acidic protein (GFAP, mouse, 1:1000;) or the neuronal-specific nuclear protein (NeuN, mouse, 1:50;) for double staining as described previously.

Statistical analysis

The data are presented as means ± SEM. For comparisons between two groups, the *P* value was evaluated and calculated using a two-tailed unpaired t-test. When there were multiple groups involved, a one-way analysis of variance (ANOVA) was used; multiple factors were compared using two-way analysis of variance (ANOVA). Values of *P* < 0.05 were considered statistically significant.

Results

Up-regulation of P2X$_4$R in the spinal cord after SNI

Compared to baseline PWMTs observed on day − 1d, SNI induced a conspicuous reduction in PWMTs ($P <$ 0.001, Fig. 1A). In contrast, no changes in the PWMTs were observed in the sham group during the observation period. To determine the expression of $P2X_4R$ in the spinal cord of SNI mice, qPCR and western-blot analysis were performed. Compared to the sham group, the SNI group showed an obvious up-regulation of $P2X_4R$ mRNA expression in the spinal cord ($P <$ 0.05, Fig. 1B). The western-blot results showed that the $P2X_4R$ protein strongly increased after nerve injury ($P <$ 0.01, Fig. 1C), which was consistent with the data from the behavioral test. As a consequence, the increased expression of $P2X_4R$ mRNA and protein in the spinal cord of SNI mice confirmed the potential ability of $P2X_4R$ to aggravate SNI-induced neuropathic pain.

The Differentially Expressed Mirnas In Neuropathic Pain Mice

To investigate the expression of miRNAs in neuropathic pain, the expression levels of miRNAs in the spinal cord of neuropathic pain mice with microarray were analyzed. Results showed 69 miRNAs were differently expressed (fold change > 2.0, $P <$ 0.05), including 46 up-regulated miRNAs (Fig. 2A) and 23 down-regulated miRNAs (Fig. 2B).

Focus on the downregulated miRNAs, we discovered that $P2X_4R$ was the target of miR-106b-5p using TargetScan software. The matched seed sequences between miR-106b-5p and $P2X_4R$ 3'UTR were highly matched between human and mice (Fig. 2C). The TargetScan software demonstrated that the seed sequence for the miR-106b-5p position (1 − 7) was paired with $P2X_4R$ 3'UTR from 363 bps to 388 bps in humans and from 1165 bps to 1190 bps in the mice. Then, the expression of miR-106b-5p in SNI mice was verified by the qPCR method, and the results were consistent with those of the microarray. MiR-106b-5p showed a down-regulation trend in the spinal dorsal horn of the SNI mice ($P <$ 0.01, Fig. 2D). To verify whether miR-106b-5p targets $P2X_4R$ 3'UTR, a dual-luciferase reporter vector containing the sequence of $P2X_4R$ 3'UTR was designed (pmirGLO $P2X_4R$ 3'UTR). When transfecting the $P2X_4R$ 3'UTR vector with three different doses of miR-106b-5p mimic (10, 20 and 50 nM) into HEK293 cells with RNAiMax, the miR-106b-5p mimic reduced relative luciferase activity in a dose-dependent manner ($P <$ 0.05, Fig. 2E).

MiR-106b-5p mimic transfection inhibits the expression of $P2X_4R$ mRNA in BV2 cells

The result was consistent with previous study [22], BV2 cells were activated after stimulating by LPS (Fig. 3A-B). Further, the cell proliferation was verified by using CCK-8 assay. The results showed that BV2 cells viability increased significantly in a dose-dependent relationship with LPS ($P <$ 0.05, Fig. 3C). Besides, miR-106b-5p mimic or inhibitor did not affect BV2 cells viability ($P >$ 0.05, Fig. 3D), which indicated miR-106b-5p mimic or inhibitor has no toxic effect on BV2 cells viability.

Moreover, to determine whether miR-106b-5p regulate the expression of $P2X_4R$, miR-106b-5p mimic was transfected in BV2 cells. LPS (2 mL, 100 ng/mL) was used to stimulate the BV2 cells 42 h later. The levels of miR-106b-5p and $P2X_4R$ mRNA were measured by qPCR, and the changes in $P2X_4R$ protein expression were determined by western-blot after transfection at 48 h. Compared to the naïve non-transfected group, LPS

stimulation induced a significant increase in P2X$_4$R at the mRNA ($P < 0.01$, Fig. 4B) and protein level ($P < 0.05$, Fig. 4C), while a reduction of miR-106b-5p was observed ($P < 0.05$, Fig. 4A). However, the overexpression of miR-106b-5p reversed the up-regulation of P2X$_4$R mRNA ($P < 0.05$, Fig. 4B) and P2X$_4$R protein ($P < 0.01$, Fig. 4C) by transfecting the miR-106b-5p mimic. Moreover, the transfection of miR-106b-5p mimic increased the expression of miR-106b-5p ($P < 0.0001$, Fig. 4A), but did not influence the changes of P2X$_4$R mRNA and protein ($P > 0.05$, Fig. 4B and 4C) in untreated BV2 cells.

In addition, we found that miR-106b-5p inhibitor transfection up-regulated P2X$_4$R mRNA ($P < 0.001$, Fig. 4E) and P2X$_4$R protein ($P < 0.01$, Fig. 4F), while it down-regulated miR-106b-5p ($P < 0.0001$, Fig. 4D). Taken together, it has been demonstrated that miR-106b-5p may suppress the expression of P2X$_4$R mRNA through its binding with P2X$_4$R 3'UTR.

P2X$_4$R are co-localized with miR-106b-5p in spinal cord of SNI mice

In order to define the localization of miR-106b-5p, the immunofluorescence in situ hybridization was performed in the spinal cord. As shown in Fig. 5, miR-106b-5p with P2X$_4$R, IBA1 (a marker for microglia cells), GFAP (a marker for glial cells), and NeuN (a marker for neurons) were stained. Results showed that miR-106b-5p was mainly co-localized with P2X$_4$R, IBA1 and NeuN, but not with GFAP.

Intrathecal miR-106b-5p agomir attenuates neuropathic pain and inhibits the expression of P2X$_4$R in the spinal cord in SNI mice

To assess the exact impact of miR-106b-5p on neuropathic pain, miR-106b-5p agomir was intrathecally delivered to SNI mice on day 7, consecutively for 3 days. As shown in Fig. 6B, qPCR results confirmed that miR-106b-5p agomir up-regulated the expression of miR-106b-5p ($P < 0.01$, Fig. 6B) in SNI mice. At day 7 after SNI, 50% paw withdrawal threshold was significantly decreased, indicating neuropathic pain was established ($P < 0.0001$, Fig. 6A). From day 3 after miR-106b-5p agomir administration, the decreased 50% paw withdrawal threshold induced by SNI were increased ($P < 0.05$, Fig. 6A), whereas the scrambled miRNA had no effect ($P > 0.05$, Fig. 6A).

Furthermore, we tested whether miR-106b-5p agomir could repress the expression of P2X$_4$R. QPCR and western-blot analysis showed that miR-106b-5p agomir reversed the up-regulation of P2X$_4$R both RNA ($P < 0.05$, Fig. 6C) and protein levels ($P < 0.001$, Fig. 6D) in SNI mice.

Intrathecal miR-106b-5p antagomir induces pain behaviors and increases the expression of P2X$_4$R in the spinal cord of naïve mice

To further explore the regulation of $P2X_4R$ by miR-106b-5p, miR-106b-5p were down-regulated in naïve mice by intrathecal injection with miR-106b-5p antagomir ($P < 0.05$, Fig. 7B). MiR-106b-5p antagomir was applied to naïve mice for 3 days and the sensitivity to the mechanical thresholds were observed. We found that the 50% paw withdrawal threshold was significantly lower in miR-106b-5p antagomir treated mice than that of scrambled miRNAs treated mice ($P < 0.01$, Fig. 7A), demonstrating that miR-106b-5p antagomir produced pain behaviors in naïve mice. Furthermore, the spinal cord tissue was harvested at day 3 to assess the expression of $P2X_4R$ at the mRNA and protein levels. As shown in Fig. 7, intrathecal miR-106b-5p antagomir increases the expression of $P2X_4R$ mRNA ($P < 0.01$, Fig. 7C), as well as $P2X_4R$ protein ($P < 0.05$, Fig. 7D) in naïve mice.

Discussion

Nervous system damage results in neuropathic pain, and miRNAs are reported to regulate neuropathic pain. In our study, $P2X_4R$ mRNA and protein were increased in the SNI mouse model. Then, 69 DE miRNAs were identified in SNI mice; among them, we also found that miR-106b-5p was decreased and that it could repress neuropathic pain development by targeting $P2X_4R$. Our findings indicated that miR-106b-5p could be used as a novel therapeutic target of neuropathic pain through regulating $P2X_4R$.

As is already known, purinergic receptor-mediated spinal microglial functions contribute significantly to pathologically enhanced pain management. [8, 9]. Consistent with previous study, the expression of spinal $P2X_4R$ was up-regulated in SNI rats and DNP rats [29−31]. Additionally, $P2X_4R$ was mostly expressed in microglial cell [32, 33]. Some researchers found that duloxetine, a drug that inhibits neurotransmitters and microglial $P2X_4R$ function and alleviates neuropathic pain after peripheral nerve injury [10]. Our results together with these findings, show that $P2X_4R$ is upregulated in neuropathic pain model, which strongly suggests that $P2X_4R$ plays a crucial role in neuropathic pain. Despite recent advances, understanding the transcriptional or translational regulatory mechanisms underlying changes in the expression and function of $P2X_4R$ under neuropathic pain conditions remains a major challenge.

MiRNAs are commonly recognized as mediators of gene expression and can serve as indicators in neuropathic pain pathophysiology [18−20]. There has been a focus on studies associated miRNAs with chronic neuropathic pain states. For example, miR-98 might depress neuropathic pain development through modulating HMGA2 [21]. MiRNAs are highly deregulated in neuropathic pain. [13, 14] and might be critical molecules for treatment. These findings provide us with information that the mechanism of $P2X_4R$ in neuropathic pain can be investigated from the perspective of miRNA.

We identified 69 miRNAs showing differential expression in the spinal cord after SNI by microarray analysis (fold change > 2, $P < 0.05$, Fig. 2A and B). Based on common mechanisms, miRNA plays a regulatory role mainly by silencing its target genes [34, 35], thus we focused on the down-regulated miRNAs in our present study. Among the down-regulated miRNAs, miR-106b-5p was found to target $P2X_4R$ through TargetScan software (Fig. 2C). Consistent with the results of the microarray, miR-106b-5p was decreased in SNI mice by the qPCR method (Fig. 2D). Interestingly, miR-106b-5p was also dysregulated in some psychiatric disorder diseases, such as Alzheimer's disease and attention-deficit hyperactivity disorder [36, 37]. Further, the dual-luciferase assay verified that miR-106b-5p negatively regulated $P2X_4R$ through combing with $P2X_4R$ 3'UTR

(Fig. 2E). Moreover, fluorescence in situ hybridization showed that miR-106b-5p was co-localized with $P2X_4R$, microglia and neurons in mice spinal cords (Fig. 4). A lot of evidence suggests that $P2X_4R$ are almost expressed in microglia to play a vital role in pain development [8, 38], but also are also expressed in DRG neurons during chronic inflammatory pain [39]. Our results are consistent with these studies and provide evidence for the interaction between miR-106b-5p and $P2X_4R$.

In our study, BV2 cells were activated after stimulating by LPS (Fig. 3A-B), which are consistent with classical theory [22]. And the viability of BV2 cells increased in a dose-dependent manner following LPS treatment ($P < 0.05$, Fig. 3C). BV2 cells are typically microglia cell lines, and $P2X_4R$ is almost exclusively expressed in microglia [10]. Further, we found that $P2X_4R$ is increased at both the mRNA and protein level under LPS-induced inflammatory conditions in BV2 cells (Fig. 4B and C). What's more, the BV2 cells transfected with miR-106b-5p mimic reversed the up-regulation of $P2X_4R$ induced by LPS (Fig. 4B and C). These data indicated that miR-106b-5p regulates $P2X_4R$ at the transcription level in BV2 cells. However, transfecting miR-106b-5p mimic did not alter the level of $P2X_4R$ in naïve BV2 cells (Fig. 4B and C, $P > 0.05$).

Further, we demonstrated that miR-106b-5p alleviated pain by inhibiting $P2X_4R$ through the changes in molecular levels in SNI mice. Meanwhile, the increased expression of $P2X_4R$ was reversed (Fig. 6C and D) with intrathecal administration of miR-106b-5p agomir in SNI mice. To further determine the role of miR-106b-5p in the SNI-induced neuropathic pain, we found that intrathecal administration of miR-106b-5p antagomir contributed to pain behaviors (Fig. 7A) and the up-regulation of $P2X_4R$ (Fig. 7C and D) in naïve mice. These results revealed that miR-106b-5p may function as an effective therapeutic target for treating neuropathic pain through regulating $P2X_4R$.

The activated $P2X_4R$ causes the phosphorylation of p38-MAPK, and the release of BDNF, all of which are essential to the persistence of pain hypersensitivity after nerve injury. Mounting evidence suggests that $P2X_4R$ may regulate the progress of neuropathic pain through the p38MAPK, ERK1/2, and PI3K/Akt pathways, which were core pathways in the development of neuropathic pain [11, 40–42]. Meanwhile, miR-106b could promote cervical cancer progression by modulating the expression of the GSK3B, VEGFA, and PTK2 genes. Importantly, these three genes play crucial roles in PI3K-Akt signaling, focal adhesion and cancer [43]. Further, the expression of miR-106b was inversely correlated with TGF-β type II receptor protein level; and miR-106b can directly inhibit the TGF-β type II receptor translation in vitro [44], while TGF-β receptor binding is an important molecular function in diabetic neuropathic pain from our previous study [27]. This accumulated evidence reveals that miR-106b-5p might regulate the expression of $P2X_4R$ in neuropathic pain through some important pathways. Therefore, further investigations illustrating the potential mechanism would provide a new direction and serviceable theoretical foundation for the clinical intervention of neuropathic pain.

Conclusion

The biological role of miR-106b-5p in neuropathic pain progression was the focus of our present research. We observed that miR-106b-5p alleviated neuropathic pain development by down-regulating $P2X_4R$. $P2X_4R$ can enable neuropathic pain development, which can be reversed by miR-106b-5p in vitro. Our data revealed that

miR-106b-5p may function as an effective therapeutic target for treating neuropathic pain through regulating P2X$_4$R.

Declarations

Authors' Contributions

H.D. (Huiying Du) and X.T. (Xinran Tan) performed the Western blot, FISH, cell culture and transfection, cell proliferation assay, luciferase assay, animal experiments and behavioral tests. H.D. and X.W. (Xuhong Wei) analyzed the data. Q.G. (Qingjuan Gong) and Z.Y (Zhongmin Yuan) designed and supervised the study. H.D. and Q.G. wrote the manuscript. All authors reviewed the manuscript.

Funding

Availability of data and materials

The datasets generated and/or analyzed in present study will be available from the corresponding author upon reasonable request from any qualified investigator.

Ethics approval and consent to participate

Not applicable.

Consent for publication

Not applicable.

Conflicts of interest

The authors report no conflicts of interest in this work.

Acknowledgements

Not applicable

References

1. Merskey H. Pain terms: a list with definitions and notes on usage. Recommended by the IASP Subcommittee on Taxonomy. Pain [Internet]. 1979 [cited 2019 Feb 11];6:249. Available from: http://www.ncbi.nlm.nih.gov/pubmed/460932.
2. Yan XT, Zhao Y, Cheng XL, He XH, Wang Y, Zheng WZ, et al. Inhibition of miR-200b/miR-429 contributes to neuropathic pain development through targeting zinc finger E box binding protein-1. J Cell Physiol. 2018;233:4815–24.
3. 10.3389/fnmol.2017.00126/full

Su S, Shao J, Zhao Q, Ren X, Cai W, Li L, et al. MiR-30b Attenuates Neuropathic Pain by Regulating Voltage-Gated Sodium Channel Nav1.3 in Rats. Front Mol Neurosci [Internet]. 2017;10:1–15. Available from: http://journal.frontiersin.org/article/10.3389/fnmol.2017.00126/full.

4. 10.1016/j.pain.2013.11.013
Van Hecke O, Austin SK, Khan RA, Smith BH, Torrance N. Neuropathic pain in the general population: A systematic review of epidemiological studies. Pain [Internet]. International Association for the Study of Pain; 2014;155:654–62. Available from: http://dx.doi.org/10.1016/j.pain.2013.11.013.

5. Stokes L, Layhadi JA, Bibic L, Dhuna K, Fountain SJ. P2 × 4 receptor function in the nervous system and current breakthroughs in pharmacology. Front Pharmacol [Internet]. 2017 [cited 2019 Feb 12];8:291. Available from: http://www.ncbi.nlm.nih.gov/pubmed/28588493.

6. Suurväli J, Boudinot P, Kanellopoulos J, Rüütel Boudinot S. P2 × 4: A fast and sensitive purinergic receptor. Biomed J [Internet]. 2017 [cited 2019 Feb 12];40:245–56. Available from: http://www.ncbi.nlm.nih.gov/pubmed/29179879.

7. Antonioli L, Blandizzi C, Fornai M, Pacher P, Lee HT, Haskó G. P2 × 4 receptors, immunity, and sepsis. Curr Opin Pharmacol [Internet]. 2019;47:65–74. Available from: https://linkinghub.elsevier.com/retrieve/pii/S147148921930013X.

8. 10.1016/j.expneurol.2011.11.012
Trang T, Beggs S, Salter MW. ATP receptors gate microglia signaling in neuropathic pain. Exp Neurol [Internet]. Elsevier Inc.; 2012;234:354–61. Available from: http://dx.doi.org/10.1016/j.expneurol.2011.11.012.

9. Inoue K, Tsuda M. Purinergic systems, neuropathic pain and the role of microglia. Exp Neurol [Internet]. 2012 [cited 2019 Feb 12];234:293–301. Available from: http://www.ncbi.nlm.nih.gov/pubmed/21946271.

10. http://dx.plos.10.1371/journal.pone.0165189
Yamashita T, Yamamoto S, Zhang J, Kometani M, Tomiyama D, Kohno K, et al. Duloxetine inhibits microglial P2 × 4 receptor function and alleviates neuropathic pain after peripheral nerve injury. Ikeda K, editor. PLoS One [Internet]. 2016 [cited 2019 Feb 18];11:e0165189. Available from: http://dx.plos.org/10.1371/journal.pone.0165189.

11. Jurga AM, Piotrowska A, Makuch W, Przewlocka B, Mika J. Blockade of P2 × 4 receptors inhibits neuropathic pain-related behavior by preventing MMP-9 activation and, consequently, pronociceptive interleukin release in a rat model. Front Pharmacol. 2017;8:1–18.

12. Gong Q, Li Y, Xin W, Zhang Y, Ren W, ie, Wei XH, et al. ATP induces long-term potentiation of C-fiber-evoked field potentials in spinal dorsal horn: The roles of P2 × 4 receptors and p38 MAPK in microglia. Glia. 2009;57:583–91.

13. 10.1016/j.bbrc.2014.12.004
Gong Q, Lu Z, Huang Q, Ruan L, Chen J, Liang Y, et al. Altered microRNAs expression profiling in mice with diabetic neuropathic pain. Biochem Biophys Res Commun [Internet]. Elsevier Inc.; 2015;456:615–20. Available from: http://dx.doi.org/10.1016/j.bbrc.2014.12.004.

14. Yang CH, Wang Y, Sims M, Cai C, He P, Yue J, et al. MiRNA203 suppresses the expression of protumorigenic STAT1 in glioblastoma to inhibit tumorigenesis. Oncotarget [Internet]. 2016 [cited 2019 Feb 12];7:84017–29. Available from: http://www.ncbi.nlm.nih.gov/pubmed/27705947.

15. Zheng Q, Cui X, Zhang D, Yang Y, Yan X, Liu M, et al. miR-200b inhibits proliferation and metastasis of breast cancer by targeting fucosyltransferase IV and α1,3-fucosylated glycans. Oncogenesis [Internet]. 2017 [cited 2019 Feb 11];6:e358–e358. Available from: http://www.ncbi.nlm.nih.gov/pubmed/28692034.

16. Liu S, Zhang F, Shugart YY, Yang L, Li X, Liu Z, et al. The early growth response protein 1-miR-30a-5p-neurogenic differentiation factor 1 axis as a novel biomarker for schizophrenia diagnosis and treatment monitoring. Transl Psychiatry [Internet]. 2017 [cited 2019 Feb 11];7:e998–e998. Available from: http://www.ncbi.nlm.nih.gov/pubmed/28072411.

17. 10.1007/s13402-016-0312-6
Guo G, Wang J, Han M, Zhang L, Li L. MicroRNA-761 induces aggressive phenotypes in triple-negative breast cancer cells by repressing TRIM29 expression. Cell Oncol [Internet]. 2017 [cited 2019 Feb 11];40:157–66. Available from: http://link.springer.com/10.1007/s13402-016-0312-6.

18. Zhang Y, Liu HL, An LJ, Li L, Wei M, Ge DJ, et al. miR-124-3p attenuates neuropathic pain induced by chronic sciatic nerve injury in rats via targeting EZH2. J Cell Biochem [Internet]. 2019 [cited 2019 Feb 11];120:5747–55. Available from: http://www.ncbi.nlm.nih.gov/pubmed/30390343.

19. 10.1016/j.neuroscience.2018.12.030
Xu L, Wang Q, Jiang W, Yu S, Zhang S. MiR-34c Ameliorates Neuropathic Pain by Targeting NLRP3 in a Mouse Model of Chronic Constriction Injury. Neuroscience [Internet]. IBRO; 2019;399:125–34. Available from: https://doi.org/10.1016/j.neuroscience.2018.12.030.

20. Wen J, He T, Qi F, Chen H. MiR-206-3p alleviates chronic constriction injury-induced neuropathic pain through targeting HDAC4. Exp Anim [Internet]. 2019 [cited 2020 May 11];68:213–20. Available from: http://www.ncbi.nlm.nih.gov/pubmed/30587671.

21. Zhang Y, Su Z, An LJ, Li L, Wei M, Ge DJ, et al. miR-98 acts as an inhibitor in chronic constriction injury-induced neuropathic pain via downregulation of high-mobility group AT-hook 2. J Cell Biochem [Internet]. 2019 [cited 2019 Feb 12];120:10363–9. Available from: http://www.ncbi.nlm.nih.gov/pubmed/30659647.

22. Hongxia L, Yuxiao T, Zhilei S, Yan S, Yicui Q, Jiamin S, et al. Zinc inhibited LPS-induced inflammatory responses by upregulating A20 expression in microglia BV2 cells. J Affect Disord [Internet]. 2019 [cited 2019 Mar 28];249:136–42. Available from: http://www.ncbi.nlm.nih.gov/pubmed/30772740.

23. Huang Y, Li Y, Wang FF, Lv W, Xie X, Cheng X. Over-Expressed miR-224 promotes the progression of cervical cancer via targeting RASSF8. PLoS One. 2016;11:e0162378.

24. Liu Z, Liang Y, Wang H, Lu Z, Chen J, Huang Q, et al. LncRNA expression in the spinal cord modulated by minocycline in a mouse model of spared nerve injury. J Pain Res. 2017;10:2503–14.

25. Morioka N, Kodama K, Tomori M, Yoshikawa K, Saeki M, Nakamura Y, et al. Stimulation of nuclear receptor REV-ERBs suppresses production of pronociceptive molecules in cultured spinal astrocytes and ameliorates mechanical hypersensitivity of inflammatory and neuropathic pain of mice. Brain Behav Immun [Internet]. 2019 [cited 2020 May 11];78:116–30. Available from: http://www.ncbi.nlm.nih.gov/pubmed/30682503.

26. 10.1016/j.neuron.2017.01.009
Yang L, Dong F, Yang Q, Yang PF, Wu R, Wu QF, et al. FGF13 Selectively Regulates Heat Nociception by Interacting with Nav1.7. Neuron [Internet]. Elsevier Inc.; 2017;93:806–21. Available from: http://dx.doi.org/10.1016/j.neuron.2017.01.009.

27. Du H, Liu Z, Tan X, Ma Y, Gong Q. Identification of the Genome-wide Expression Patterns of Long Non-coding RNAs and mRNAs in Mice with Streptozotocin-induced Diabetic Neuropathic Pain. Neuroscience [Internet]. IBRO; 2019;402:90–103. Available from: https://linkinghub.elsevier.com/retrieve/pii/S0306452218308583.

28. 10.1038/cddis.2016.465
Wu Y, Ma S, Xia Y, Lu Y, Xiao S, Cao Y, et al. Loss of GCN5 leads to increased neuronal apoptosis by upregulating E2F1- and Egr-1-dependent BH3-only protein Bim. Cell Death Dis [Internet]. Nature Publishing Group; 2017;8:e2570-17. Available from: http://dx.doi.org/10.1038/cddis.2016.465.

29. Wang Z, Mei W, Wang Q, Guo R, Liu P, Wang Y, et al. Role of dehydrocorybulbine in neuropathic pain after spinal cord injury mediated by P2 × 4 receptor. Mol Cells [Internet]. 2019 [cited 2019 Feb 17];42:143–50. Available from: http://www.ncbi.nlm.nih.gov/pubmed/30622226.

30. Zhou TT, Wu JR, Chen ZY, Liu ZX, Miao B. Effects of dexmedetomidine on P2 × 4Rs, p38-MAPK and BDNF in spinal microglia in rats with spared nerve injury. Brain Res [Internet]. 2014 [cited 2019 Feb 17];1568:21–30. Available from: http://www.ncbi.nlm.nih.gov/pubmed/24792496.

31. Teixeira JM, dos Santos GG, Neves AF, Athie MCP, Bonet IJM, Nishijima CM, et al. Diabetes-induced Neuropathic Mechanical Hyperalgesia Depends on P2 × 4 Receptor Activation in Dorsal Root Ganglia. Neuroscience. 2019;398:158–70.

32. Chun BJ, Stewart B, Vaughan D, Bachstetter A, Kekenes-Huskey P. Simulation of P2X-mediated calcium signalling in microglia. J Physiol [Internet]. 2019 [cited 2019 Feb 18];597:799–818. Available from: http://www.ncbi.nlm.nih.gov/pubmed/30462840.

33. 10.1124/mol.118.113696
Dhuna K, Felgate M, Bidula SM, Walpole S, Bibic L, Cromer BA, et al. Ginsenosides act as positive modulators of P2 × 4 receptors. Mol Pharmacol [Internet]. 2019 [cited 2019 Feb 18];95:210–21. Available from: http://molpharm.aspetjournals.org/lookup/doi/10.1124/mol.118.113696.

34. El Bezawy R, Tinelli S, Tortoreto M, Doldi V, Zuco V, Folini M, et al. MiR-205 enhances radiation sensitivity of prostate cancer cells by impairing DNA damage repair through PKCϵ and ZEB1 inhibition. J Exp Clin Cancer Res [Internet]. 2019 [cited 2019 Feb 18];38:51. Available from: http://www.ncbi.nlm.nih.gov/pubmed/30717752.

35. Zhou Y, Huang T, Siu HL, Wong CC, Dong Y, Wu F, et al. IGF2BP3 functions as a potential oncogene and is a crucial target of miR-34a in gastric carcinogenesis. Mol Cancer [Internet]. 2017 [cited 2019 Feb 18];16:77. Available from: http://www.ncbi.nlm.nih.gov/pubmed/28399871.

36. 10.1016/j.jpsychires.2018.12.013
Zadehbagheri F, Hosseini E, Bagheri-Hosseinabadi Z, Rekabdarkolaee HM, Sadeghi I. Profiling of miRNAs in serum of children with attention-deficit hyperactivity disorder shows significant alterations. J Psychiatr Res [Internet]. Elsevier Ltd; 2019;109:185–92. Available from: https://doi.org/10.1016/j.jpsychires.2018.12.013.

37. Rahman MR, Islam T, Turanli B, Zaman T, Faruquee HM, Rahman MM, et al. Network-based approach to identify molecular signatures and therapeutic agents in Alzheimer's disease. Comput Biol Chem [Internet]. 2019 [cited 2020 May 11];78:431–9. Available from: http://www.ncbi.nlm.nih.gov/pubmed/30606694.

38. 10.1016/j.coph.2019.02.001

Inoue K. Role of the P2 × 4 receptor in neuropathic pain. Curr Opin Pharmacol [Internet]. Elsevier Ltd; 2019;47:33–9. Available from: https://doi.org/10.1016/j.coph.2019.02.001.

39. Lalisse S, Hua J, Lenoir M, Linck N, Rassendren F, Ulmann L. Sensory neuronal P2RX4 receptors controls BDNF signaling in inflammatory pain. Sci Rep. 2018;8:1–12.

40. 10.1016/j.brainresbull.2018.07.003
    Deng Z, Li C, Liu C, Du E, Xu C. Catestatin is involved in neuropathic pain mediated by purinergic receptor P2 × 4 in the spinal microglia of rats. Brain Res Bull [Internet]. Elsevier; 2018;142:138–46. Available from: https://doi.org/10.1016/j.brainresbull.2018.07.003.

41. Guo J, Wang H, Jin X, Jia D, Zhou X, Tao Q. Effect and mechanism of inhibition of PI3K/Akt/mTOR signal pathway on chronic neuropathic pain and spinal microglia in a rat model of chronic constriction injury. Oncotarget [Internet]. 2017;8:52923–34. Available from: http://www.ncbi.nlm.nih.gov/pubmed/28881783%0Ahttp://www.pubmedcentral.nih.gov/articlerender.fcgi?artid=PMC5581082.

42. 10.1016/j.lfs.2018.07.026
    Shao J, Xu R, Li M, Zhao Q, Ren X, Li Z, et al. Glucocorticoid receptor inhibit the activity of NF-κB through p38 signaling pathway in spinal cord in the spared nerve injury rats. Life Sci [Internet]. Elsevier Inc; 2018;208:268–75. Available from: https://doi.org/10.1016/j.lfs.2018.07.026.

43. Yi Y, Liu Y, Wu W, Wu K, Zhang W. The role of miR-106p-5p in cervical cancer: from expression to molecular mechanism. Cell Death Discov [Internet]. 2018 [cited 2020 May 13];4:94. Available from: http://www.nature.com/articles/s41420-018-0096-8.

44. Ren J, Zhang J, Xu N, Han G, Geng Q, Song J, et al Signature of Circulating MicroRNAs as Potential Biomarkers in Vulnerable Coronary Artery Disease. Beltrami AP, editor. PLoS One [Internet]. 2013 [cited 2020 May 11];8:e80738. Available from: http://www.ncbi.nlm.nih.gov/pubmed/24339880.
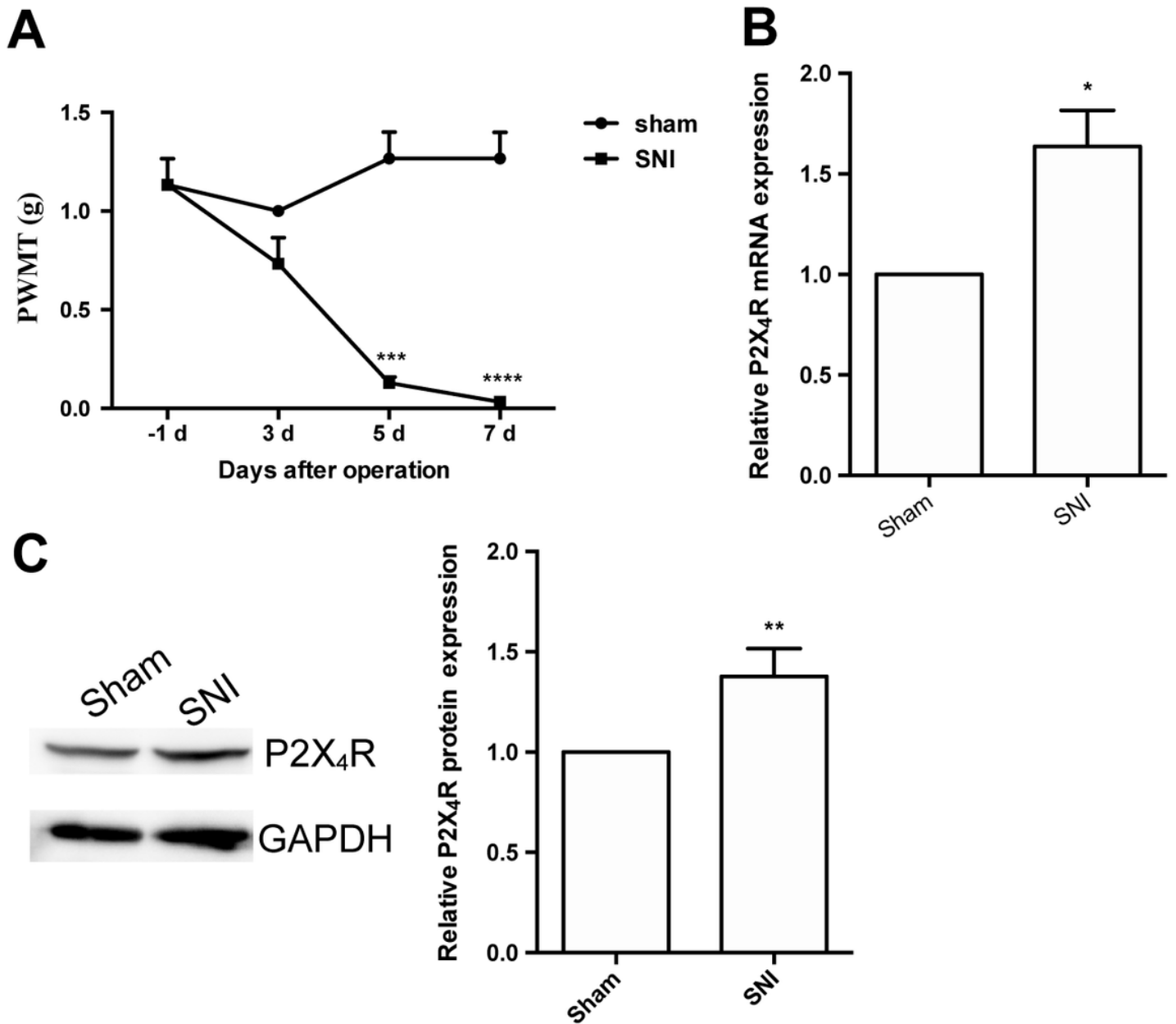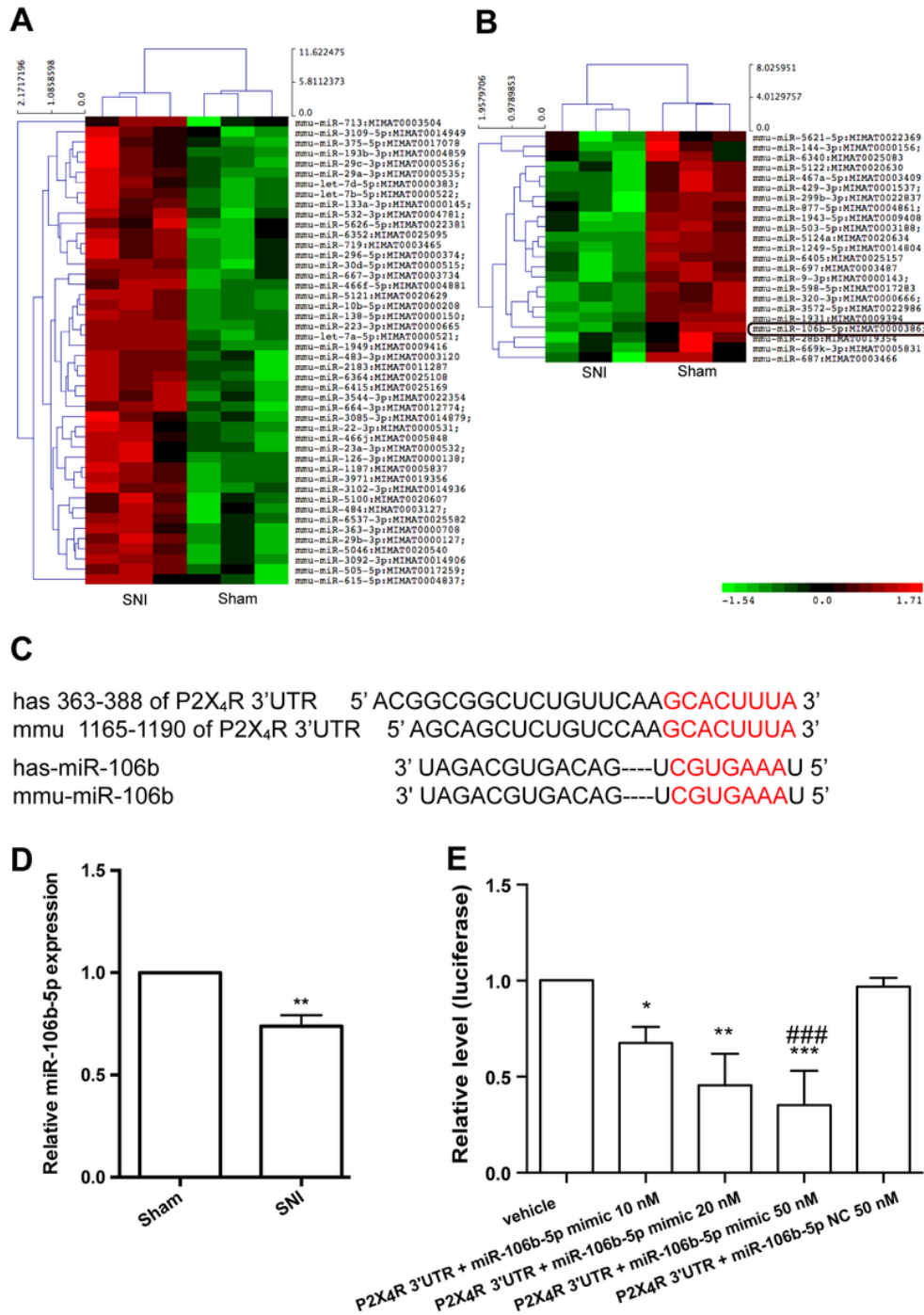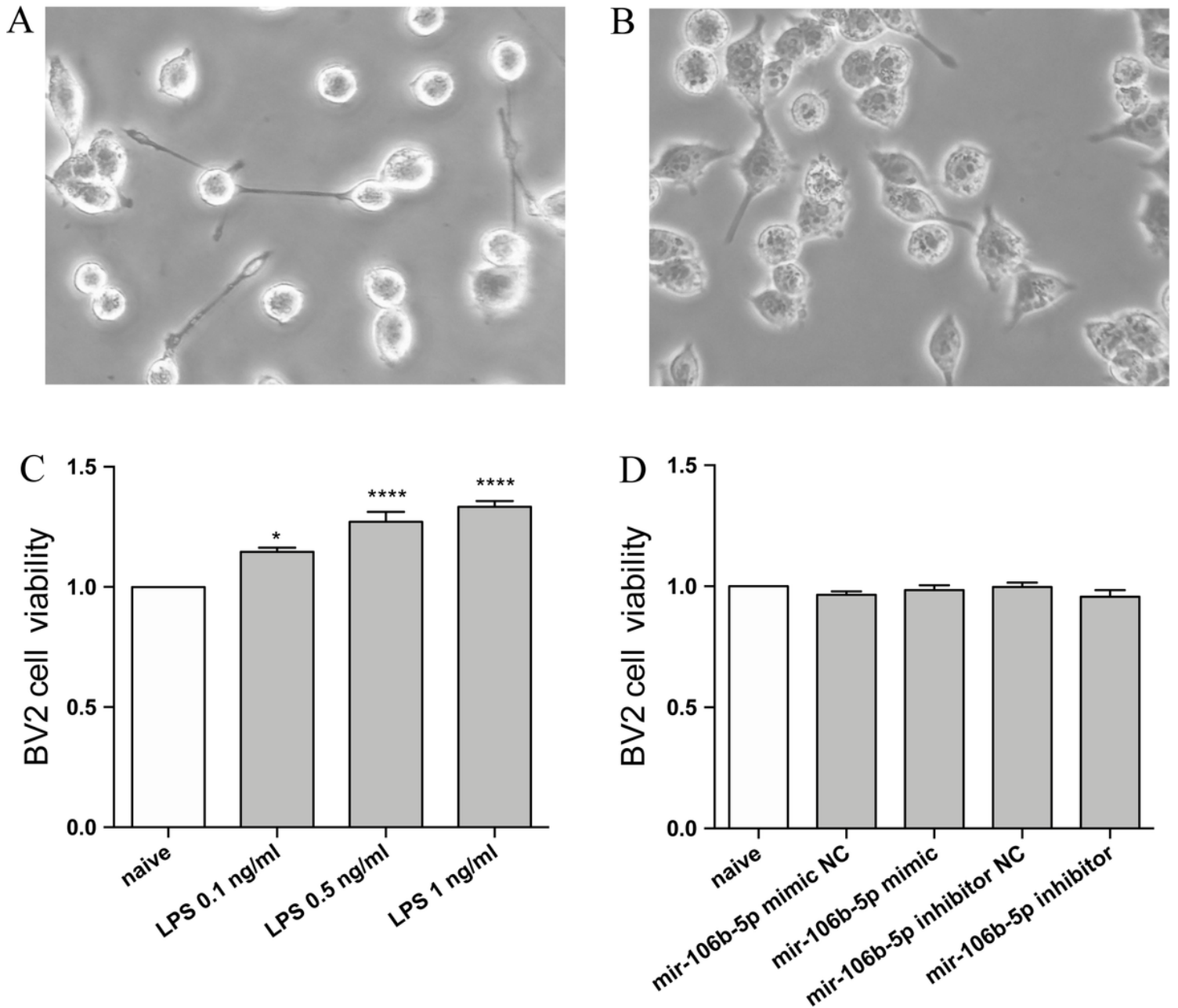
Figures

Figure 1

The pain behavior of neuropathic pain induced by SNI and the change in expression of P2X4R mRNA and protein. (A) Responses of the paw to mechanicals. *** P < 0.001, **** P < 0.0001 vs. sham. Two-way ANOVA, n = 6 mice. (B) The increased expression of P2X4R mRNA in the spinal cord of SNI mice. t4 = 3.539, * P < 0.05, n = 3 mice. (C) The increased expression of P2X4R protein in the spinal cord of SNI mice. t4 = 4.670, ** P < 0.01. Two-tailed unpaired t-test, n = 3 mice.

Figure 2

MiR-106b-5p was downregulated in neuropathic pain induced by SNI, and miR-106b-5p directly targets P2X4R 3'UTR. (A-B) The heat map showed the differential expression of miRNA in SNI mice (fold change > 2.0, P < 0.05). (C) The matched seed region between miR-106b-5p and P2X4R 3'UTR predicted by software in red. (D) The decreased expression of miR-106b-5p in the spinal cord of SNI mice. Two-tailed unpaired t-test, t4 = 4.862, ** P < 0.01, n = 3 mice. (E) Transfection of miR-106b-5p mimic with wild-type P2X4R 3'UTR plasmid vector reduced relative luciferase activity, but no change in luciferase activity was detected in the scramble group, * P < 0.05, ** P < 0.01, *** P < 0.01 vs. vehicle, ### P < 0.001 vs. scramble. One-way ANOVA, n = 3.
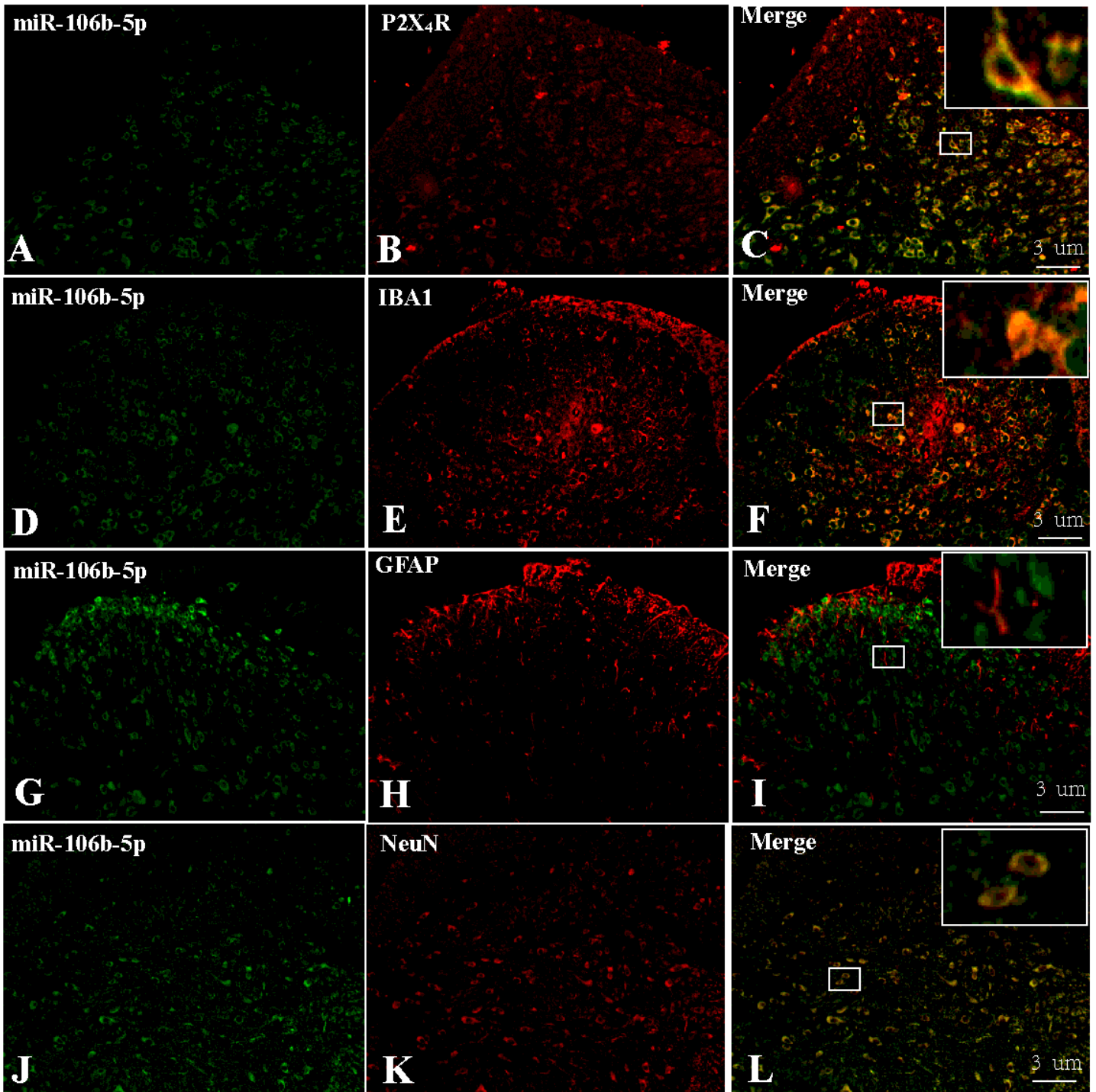
Figure 3

Morphology of BV2 cells observed under microscope and effect of LPS or miR-106b-5p mimic or inhibitor on BV2 microglia cell viability. (A) The picture shows normal morphology of BV2 cells. (B) The picture presents the morphology of LPS-stimulated BV2 cells. (C) Cell viability was evaluated ty CCK-8 assay. The affection of LPS on cell growth was denoted as a percentage of normal control, ** $P < 0.05$, **** $P < 0.0001$ vs. naïve. One-way ANOVA, n = 8. (D) Compared with naïve group, the affection of those compounds on cell growth showed no different. $P > 0.05$, One-way ANOVA, n = 5.
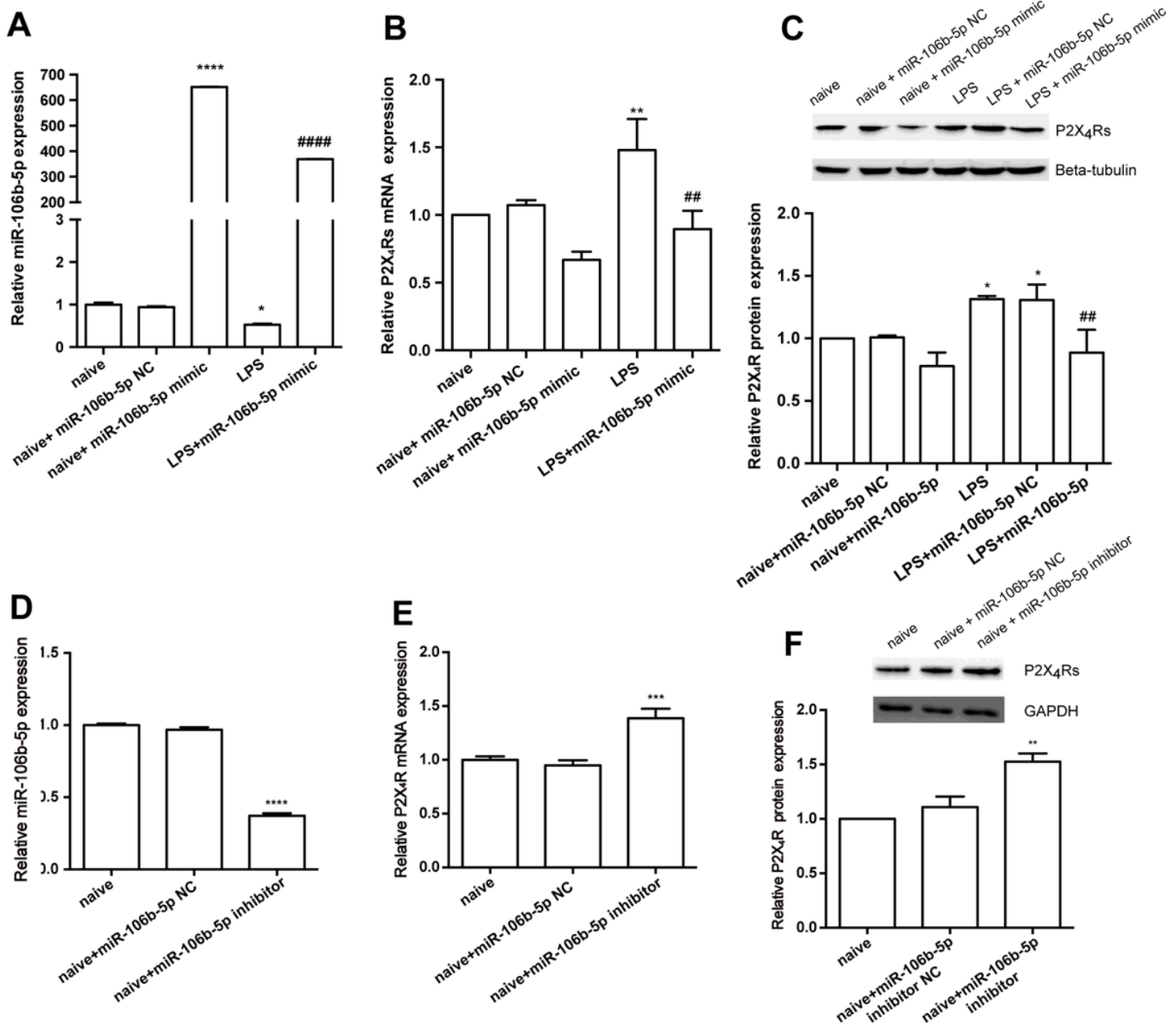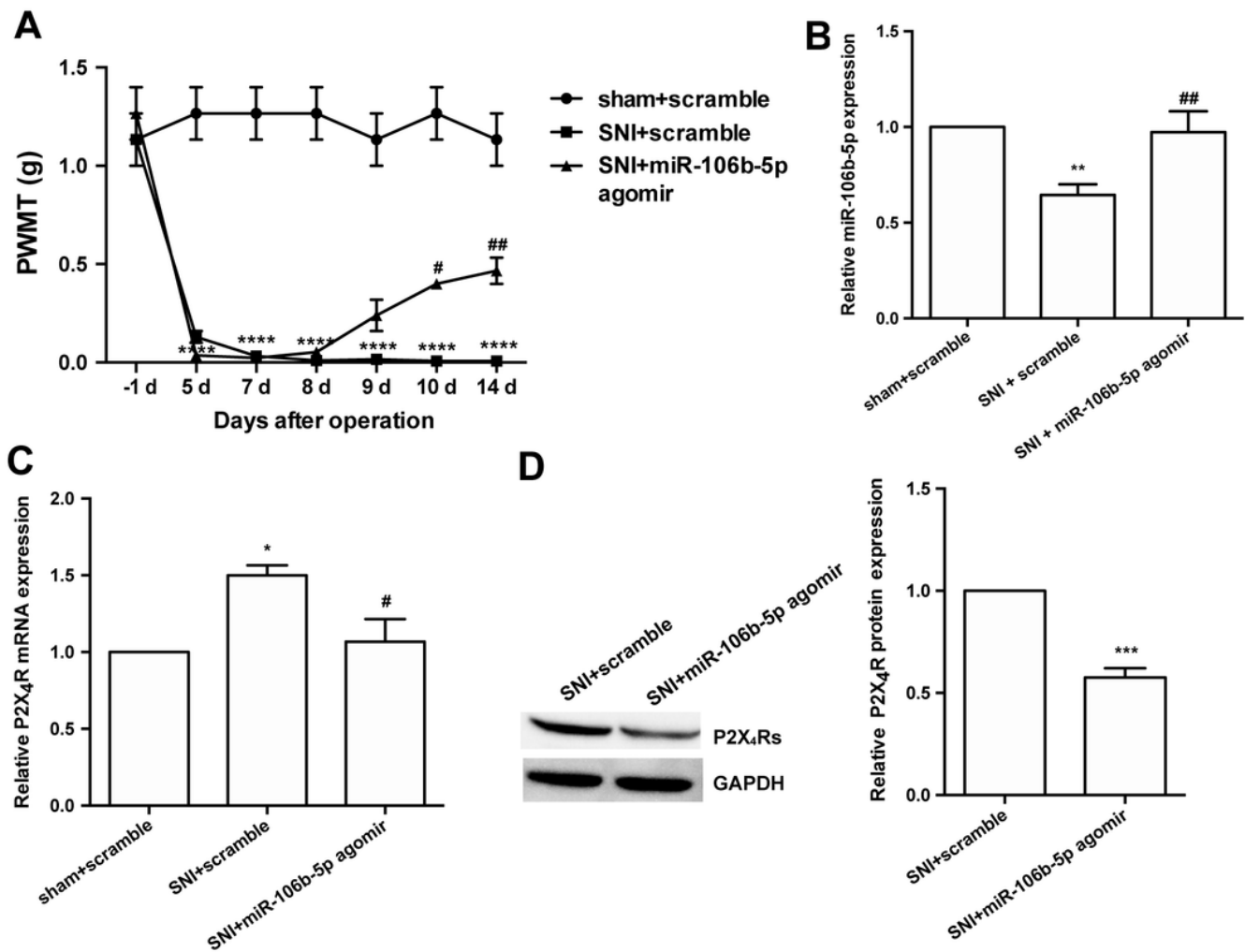
Figure 4

MiR-106b-5p regulated the expression of P2X4R in BV2 cells. (A-C) The relative expression of miR-106b-5p (A) and P2X4R mRNA (B) and protein (C) treated with miR-106b-5p mimic/scramble in BV2 cells. * P < 0.05, ** P < 0.01, **** P < 0.0001 vs. naïve; ## P < 0.01, #### P < 0.0001 vs. LPS. One-way ANOVA, n = 3 mice. (D-F) The relative expression of miR-106b-5p (D) and P2X4R mRNA (E) and protein (F) treated with miR-106b-5p inhibitor/scramble in BV2 cells. ** P < 0.01, *** P < 0.001, **** P < 0.0001 vs. naïve. One-way ANOVA, n = 3 mice.
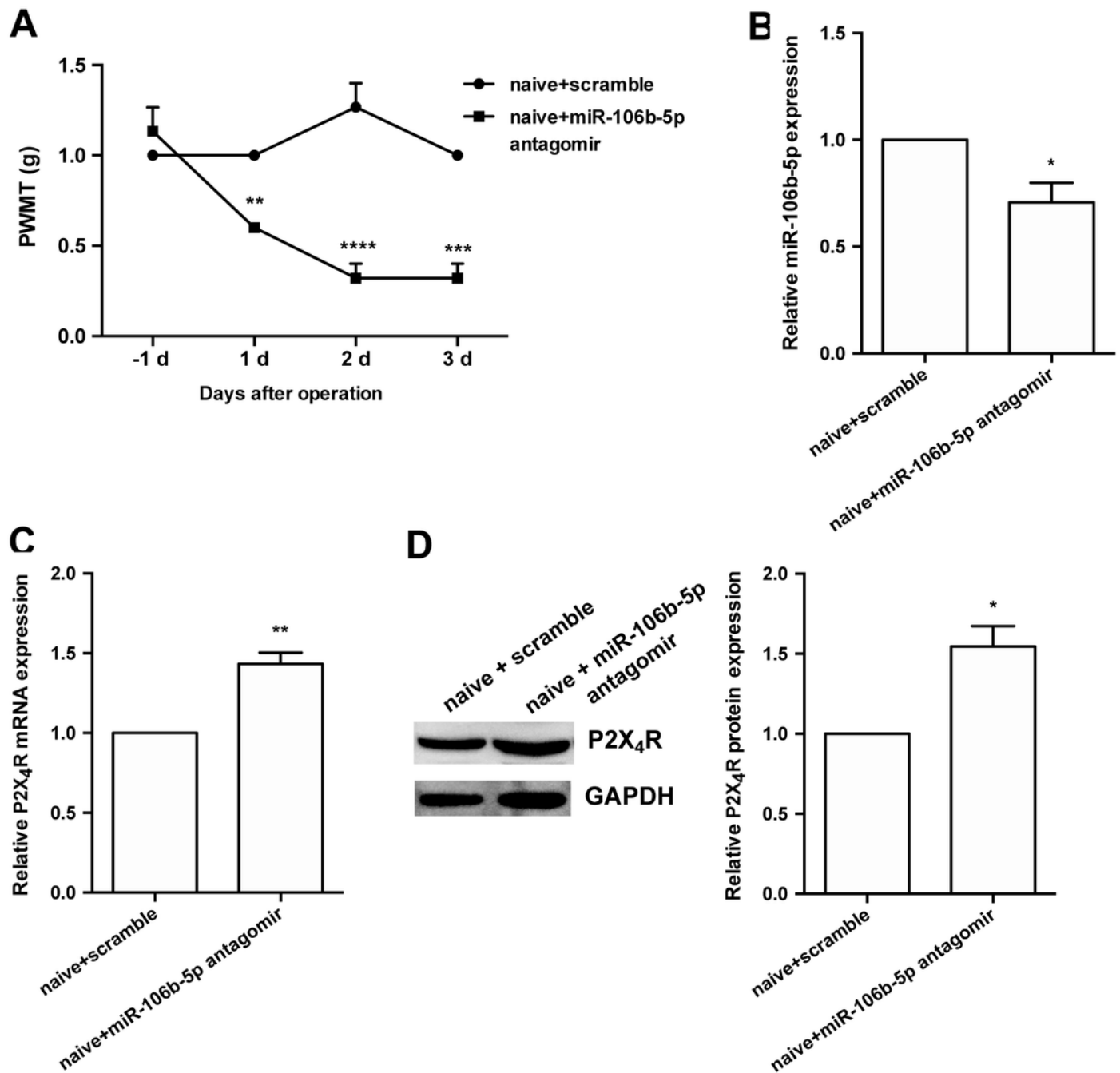
Figure 5

MiR-106b-5p regulated the expression of P2X4R in BV2 cells. (A-C) The relative expression of miR-106b-5p (A) and P2X4R mRNA (B) and protein (C) treated with miR-106b-5p mimic/scramble in BV2 cells. * P < 0.05, ** P < 0.01, **** P < 0.0001 vs. naïve; ## P < 0.01, #### P < 0.0001 vs. LPS. One-way ANOVA, n = 3 mice. (D-F) The relative expression of miR-106b-5p (D) and P2X4R mRNA (E) and protein (F) treated with miR-106b-5p inhibitor/scramble in BV2 cells. ** P < 0.01, *** P < 0.001, **** P < 0.0001 vs. naïve. One-way ANOVA, n = 3 mice.

Figure 6

MiR-106b-5p agomir down regulated P2X4R and alleviated neuropathic pain. (A) The paw mechanicals withdraw thresholds were tested in mice. **** $P < 0.0001$ vs. sham + scramble; # $P < 0.05$, ## $P < 0.01$ vs. SNI + scramble. Two-way ANOVA, n = 6 mice. (B-C) The relative expression of miR-106b-5p (B) and P2X4R mRNA (C) with intrathecal miR-106b-5p agomir/scramble in the spinal cord of SNI mice was determined by qPCR. * $P < 0.05$, ** $P < 0.01$ vs. sham + scramble; # $P < 0.05$, ## $P < 0.01$ vs. SNI + scramble. One-way ANOVA, n =3 mice . (D) P2X4R protein expression in the spinal cord of SNI mice at 14 days injected with intrathecal miR-106b-5p agomir, $t4 = 9.357$, *** $P < 0.001$. Two-tailed unpaired t-test, n = 3 mice.

Figure 7

P2X4R was upregulated by miR-106b-5p antagomir with pain behavior. (A) The paw mechanicals withdraw thresholds were tested in mice. ** P <0.01, *** P <0.001, **** P < 0.0001 vs naïve + scramble. Two-way ANOVA, n = 3 mice. (B) The relative expression of miR-106b-5p at 3 days in the spinal cord of mice, t4 = 3.213, * P < 0.05. (C) The relative expression of P2X4R mRNA at 3 days in the spinal cord of mice, t4 = 6.151, ** P < 0.01. (D) The relative expression of P2X4R protein at 3 days in the spinal cord of mice, t4 = 4.330, * P < 0.05. Two-tailed unpaired t-test, n = 3 mice.